Journal of Engineering and Technology for Industrial Applications

ISSN ONLINE: 2447-0228

ITEGAM-JETIA

Manaus, v.11 n.56, p.296-309. November/December, 2025.

DOI: https://doi.org/10.5935/jetia. v11i56.2772

RESEARCH ARTICLE OPEN ACCESS

ENHANCED CONTROL AND ANALYSIS OF A FIVE-LEG INVERTER USING PWM STRATEGIES FOR DUAL ASYNCHRONOUS MOTOR DRIVES

Oussama Sait*[1], Samia Latreche[2], Belkacem Sait[3], Mabrouk Khemliche[4], Hamza Khemliche[5]

[1, 2, 3,4]Automatic Laboratory of Setif-LAS, Automatic and Smart Systems Department, University of Ferhat Abbas Setif 1, Setif, Algeria.
[5]Reaserch Center In Industrial Technologies CRTI, P.O. box 64, Cheraga 16014, Algiers, Algeria.

[1]https://orcid.org/0009-0006-0662-1387, [2]https://orcid.org/0000-0002-1496-739X, [3]https://orcid.org/0009-0005-9379-4763
[4]https://orcid.org/0000-0003-2638-6688, [5]https://orcid.org/0000-0002-7373-780X.

Email: *sait.oussama@univ-setif.dz , ksamia2002@yahoo.fr, belkacemsait@yahoo.fr, mabroukkhemliche@univ-setif.dz, h.khemliche@crti.dz

ARTICLE INFO

Article History
Received: October 3, 2025
Revised: November 20, 2025
Accepted: December 1, 2025
Published: September 31, 2025

Keywords:
Five-leg inverter,
Dual motor drive,
PWM,
Indirect vector control,
Harmonic distortion,
Matlab/Simulink.

ABSTRACT

This study offers a detailed control strategy and performance assessment of a five-leg inverter configuration designed for the autonomous operation of two three-phase induction motors. Traditional dual-motor drive systems generally utilize two distinct three-leg inverters, leading to heightened hardware complexity, elevated costs, and greater spatial demands. The suggested five-leg inverter architecture mitigates these restrictions by employing a shared leg between two motor phases, so decreasing the number of power switching devices while preserving complete independent control of both motors. The system functions by sinusoidal Pulse Width Modulation (PWM) integrated with sophisticated indirect vector control techniques. A comprehensive simulation model in MATLAB/Simulink evaluates system performance under balanced load settings, examining critical metrics including voltage waveforms, torque response, and harmonic distortion for each motor. The findings indicate that the five-leg inverter facilitates steady, decoupled motor performance characterized by minimal harmonic distortion and rapid dynamic response. A comparative assessment with a traditional six-leg inverter architecture demonstrates that the suggested topology provides comparable performance while minimizing component count and complexity. This study confirms the practicality and benefits of shared-leg inverter configurations for multi-motor drives, facilitating more compact, economical, and efficient solutions in industrial motor control applications.

I. INTRODUCTION

Multi-motor drive systems have become increasingly important in industrial automation, electric vehicles, and robotics, where the need for both independent and coordinated motor control is essential [1]. Traditionally, each motor has been driven by a separate three-phase inverter, resulting in increased hardware complexity, elevated costs, and larger system dimensions [2]. In response to these limitations, multi-leg inverter topologies have been introduced as compact and economically viable alternatives. The five-leg inverter topology has garnered considerable interest for its capacity to power two three-phase motors utilising merely five legs, as it allows for the sharing of one common leg between the two drives [3]. This configuration leads to a reduction in the number of switching devices and gate drivers by approximately 16–33% when compared to traditional dual-inverter systems [4]. Nevertheless, this topology presents various control challenges, especially in relation to the modulation of the shared leg, which must guarantee decoupled operation of both machines while preventing inter-phase interference [5]. To address this challenge, advanced PWM methods like sinusoidal PWM (SPWM) are widely used, along with vector control strategies to maintain steady torque and flux responses. A series of investigations have examined the performance of five-leg inverters across diverse load conditions [6], [7]. However, a significant gap exists in the literature regarding comprehensive comparative analyses of five-leg and six-leg inverters, particularly concerning harmonic distortion,

dynamic performance, and switching behaviour. Furthermore, many current studies fail to adequately assess the influence of the shared-leg configuration on torque ripple and the system's overall stability. This investigation aims to fill the existing gap by delivering a thorough simulation-based performance evaluation of a five-leg inverter that drives two asynchronous machines, employing sinusoidal pulse width modulation and indirect vector control methodologies. A comparative analysis with a conventional six-leg inverter has been performed to assess the performance trade-offs and substantiate the proposed architecture.

This work presents the following contributions:

- A detailed simulation model of a five-leg inverter was developed using MATLAB/Simulink.
- Assessment of dual-motor operation performance concerning voltage, torque, and harmonic content.
- A comparative analysis involving a six-leg inverter to illustrate the advantages of the shared-leg topology.

The findings offer novel perspectives on the practicality and constraints of shared-leg inverter configurations for multi-motor systems, especially in contexts where hardware simplicity and compactness are emphasized.

II. RELATED WORK

Several research initiatives have explored multi-motor drive systems and inverter configurations designed to minimize hardware complexity while ensuring efficient motor control. The traditional approach of employing two independent three-leg inverters has been extensively examined and applied, owing to its simple design and established reliability [8]. Nevertheless, this methodology intrinsically leads to a greater number of components, elevated switching losses, and an expanded requirement for installation space [9]. In response to these challenges, configurations utilizing shared-leg inverters have been developed. The five-leg inverter has emerged as a compact alternative, demonstrating its ability to control two three-phase motors while utilizing fewer switching devices [10]. This configuration minimizes the quantity of power semiconductor switches and gate drivers, resulting in a significant enhancement in power density and the overall system cost [11]. A range of modulation techniques has been proposed for the five-leg inverter. Sinusoidal PWM (SPWM) exhibits commendable performance in terms of voltage quality and ease of implementation [12]. Nevertheless, the ability to ensure fully decoupled operation for both motors through the shared leg remains a subject of ongoing research. Alternative methods, such as space vector PWM (SVPWM) and hybrid modulation, have been examined with the aim of minimizing harmonic content and torque ripple [13], [14].

The implementation of indirect rotor flux-oriented vector control has demonstrated efficacy in sustaining stable torque and flux responses within dual-motor systems [15]. Several studies have incorporated this methodology alongside advanced control techniques, including fuzzy logic and model predictive control, to improve robustness in the face of varying load conditions [16]. Despite these advancements, there remains a notable lack of studies that offer a comprehensive comparison between five-leg and six-leg inverter topologies under the same operating conditions. A considerable body of research emphasizes the reduction of hardware or conducts isolated case analyses, often neglecting the critical need to benchmark these methodologies against established frameworks [17]. Moreover, the existing literature rarely provides thorough harmonic analysis or dynamic performance evaluations, both of which are crucial for validating the practical significance of shared-leg configurations [18]. This investigation seeks to address the existing research gap through a simulation-based comparative analysis of five-leg and six-leg inverters, with particular emphasis on waveform quality, system response, and harmonic distortion. The proposed work presents a systematic evaluation framework and elucidates the trade-offs and advantages of shared-leg inverters in dual-drive applications.

III. THEORETICAL FRAMEWORK

III.1 SIX-LEG INVERTER TOPOLOGY

A six-leg inverter is a multiphase inverter consisting of six power switches, commonly MOSFETs or IGBTs, organized in a three-phase configuration to manage multiple electrical machines. The configuration of the six-leg inverter comprises six switching devices, with each device assigned to a particular leg of the inverter. The six terminals generate three-phase outputs tailored for the respective load, generally organized in a balanced configuration, with each phase output being regulated autonomously. This topology is characterized by the independent management of each phase leg, which markedly enhances voltage regulation and fault tolerance relative to conventional three-phase inverters[19]. The modulation scheme utilized dictates the switching function in a six-leg inverter. In pulse width modulation (PWM), switching devices are engaged and disengaged at a high frequency, thereby controlling the voltage output through adjustments to the duty cycle of the switches.

Each of the six legs is equipped with a corresponding switching signal, with the switching frequency and duty cycle carefully calculated to ensure a balanced and stable output voltage. This architecture promotes redundancy, thereby ensuring fault tolerance in the event of a failure in one of the switching devices. In the occurrence of a fault in one leg, the inverter can be replaced, allowing the system to continue functioning with reduced performance, thereby preventing complete failure [20]. The core functionality of the six-leg inverter is predicated on the synthesis of sinusoidal pulse width modulation (SPWM) and space vector modulation (SVM) techniques. The modulation techniques employed facilitate the six-leg inverter's generation of requisite three-phase voltage waveforms, characterized by minimal harmonic distortion and enhanced efficiency. The voltage vectors are generated through the sequential switching of the six legs to accurately depict the intended output voltage vector. Meanwhile, the modulation strategy improves the inverter's efficiency by minimizing switching losses and harmonics.

III.2 FIVE-LEG INVERTER TOPOLOGY

An innovative adaption of the six-leg inverter, the five-leg inverter reduces switch count while guaranteeing fault tolerance and multiple motor control. The five-legged arrangement uses five power switches and a shared leg for two motors. Reducing the number of switches makes the solution more efficient and cost-effective while keeping some key six-leg inverter benefits. In this setup, one inverter leg connects the two motors, while the other four legs regulate their voltage. A shared leg between the motors defines the five-leg inverter. This design reduces system components and allows machines to operate autonomously. This design minimizes switches and components compared to a six-leg system, which is beneficial in space- and cost-constrained scenarios [21]. Though using fewer switching signals, the five-leg inverter's switching functions are similar to those of the six-leg inverter. The common leg is usually the motors' neutral point, and the switching pattern balances each motor's voltage. PWM is used to provide switching signals for the five-leg inverter, allowing it to be controlled and its output voltages changed. The five-leg inverter can use fault-tolerant tactics such switching reconfiguration to minimize problems in one leg, guaranteeing system continuity. [22][23].

III.3 CONTROL SIGNAL DEFINITION

The control signals for the five-arm inverter are articulated through mathematical expressions that are derived from the modulation techniques employed in the switching devices. The primary aim is to produce suitable switching pulses for each leg of the inverter, which will yield the intended voltage waveforms for the associated motors. In a conventional PWM-controlled inverter, the duty cycle of the switching signals is determined by the desired output voltage and the modulation technique employed [24]. Define the voltage references for the phases as Vref,a, Vref,b, and Vref,c for the three-phase motors, with each reference voltage being contingent upon the desired output voltage and the modulation technique employed. The control signals Sa, Sb, and Sc corresponding to the three phases can be articulated as follows:

$$\mathrm{Sa(t)} = \mathrm{PWM\ (Vref, a, t)} \tag{1}$$

$$\mathrm{Sb(t)} = \mathrm{PWM\ (Vref, b, t)} \tag{2}$$

$$\mathrm{Sc(t)} = \mathrm{PWM\ (Vref, c, t)} \tag{3}$$

The function PWM(Vref,t) delineates the pulse width modulation mechanism, which modulates the duty cycle of the switches to produce the desired voltage waveform. The duty cycle D for each phase is determined by the reference voltage and the modulation technique, generally articulated as follows:

$$\mathrm{D} = \mathrm{Vref\ VDC} \tag{4}$$

In this context, VDC refers to the voltage present on the DC bus. The generation of the switching signal occurs through the comparison of the reference voltage against a triangular carrier signal. When the reference voltage surpasses the carrier signal, the switch activates; if not, it remains deactivated. In the context of a five-leg inverter, the control signals for the common leg S common are established with consideration to voltage balancing and the configuration of shared power. The implementation of the switching strategy for the common leg guarantees that the voltage at the common point is maintained in a stable and balanced manner between the two motors. This requires careful calculation of the switching pulses for the common leg, along with the other legs, to achieve the desired system performance.The mathematical formulations related to the control signals in a five-leg inverter can be succinctly expressed as follows:

$$\mathrm{Scommon(t)} = \mathrm{PWM\ (Vcommon, t)} \tag{5}$$

The variable V common denotes the voltage at the common leg, while the PWM function guarantees that this voltage is maintained in a balanced state concerning the phases linked to the motors. The comprehensive control system is meticulously engineered to ensure a stable and balanced voltage supply to each motor while concurrently minimizing switching losses and harmonic distortion [25].

IV. SYSTEM ARCHITECTURE AND CONTROL STRATEGY

The proposed system utilizes a five-leg inverter to regulate two three-phase asynchronous motors, effectively reducing the number of necessary switching devices. This topology decreases the total number of legs from six to five by incorporating a shared leg between the third phases of both motors, in contrast to traditional configurations that employ two distinct three-leg inverters. This leads to lower hardware expenses, improved power density, and refined control circuitry, rendering the system appealing for compact and economical applications [26]. The system architecture is shown in Figure 1. uses separate vector control loops for each motor, generating voltage references that feed a centralized sinusoidal PWM. The PWM drives the five-leg inverter, which supplies modulated voltages to both motors, while current and speed feedback ensure real-time adjustment and stability.

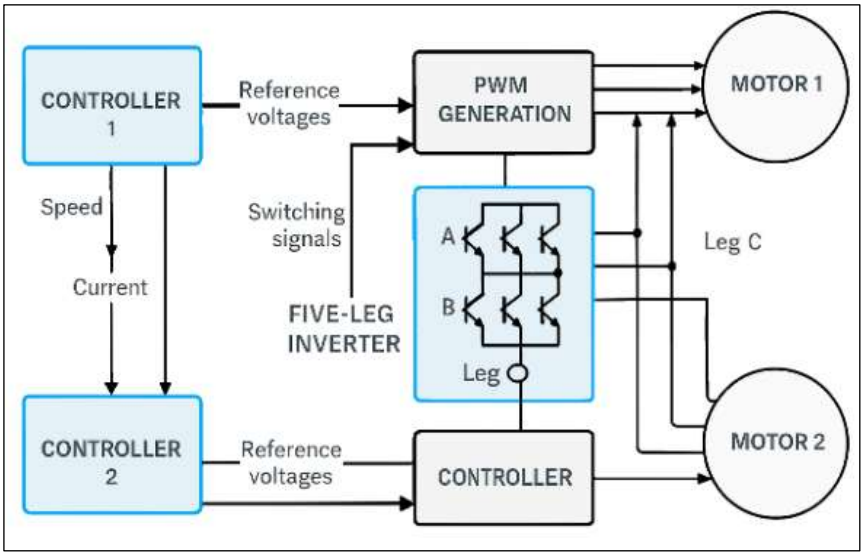

Figure 1: System architecture of the proposed five-leg inverter system.
Source: Authors, (2025).

The inverter configuration allocates two legs for each motor while sharing a central leg between both machines. Figure 2 illustrates that Legs A and B deliver phases a_1 and b_1 for Motor 1 (M1), whereas Legs D and E supply phases a_2 and b_2 for Motor 2 (M2). Leg C is concurrently linked to phases c_1 and c_2 of both motors. Synchronizing the switching signals on this common leg is crucial to prevent coupling effects and ensure control independence [27], [28].

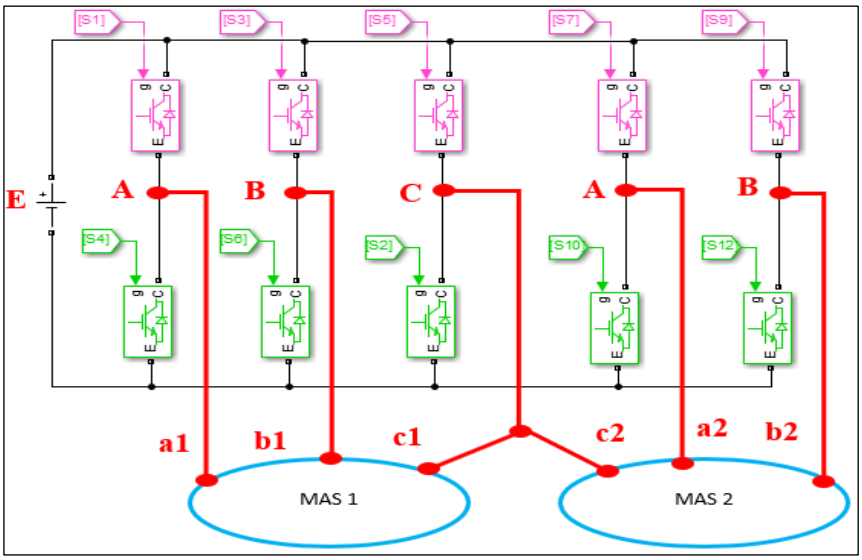

Figure 2: Electrical structure of the five-leg inverter supplying two three-phase asynchronous motors.
Source: Authors, (2025).

IV.1 PWM CONTROL SIGNALS AND GATE LOGIC

A sinusoidal Pulse Width Modulation (SPWM) approach is utilized to produce the requisite gate signals for the inverter switches. This technique entails juxtaposing sinusoidal reference voltages with a triangular carrier waveform to generate high-frequency switching pulses. The simplicity, convenience of digital implementation, and adequate harmonic performance render SPWM appropriate for multi-motor applications. In a five-leg inverter, the modulation technique must guarantee synchronized control of the shared leg to avert conflicting operations [29]. In order to implement the SPWM switching logic, the generation of control signals is based on the comparison between sinusoidal voltage references and a high-frequency sawtooth waveform. This process is illustrated in Figures 3 through 5. Figure 3 presents the three-phase sinusoidal voltages overlaid on a sawtooth generator signal, which determines the instant of switching by the point of intersection. Figure 4 shows the individual sine and sawtooth waveforms for a single phase to highlight their relative dynamics. Figure 5 displays the resulting summation used to define the pulse timing. This approach is foundational in defining the modulation index and duty cycle of each inverter leg, ensuring harmonic balance and time-aligned switching even in the five-leg configuration shared by two motors.

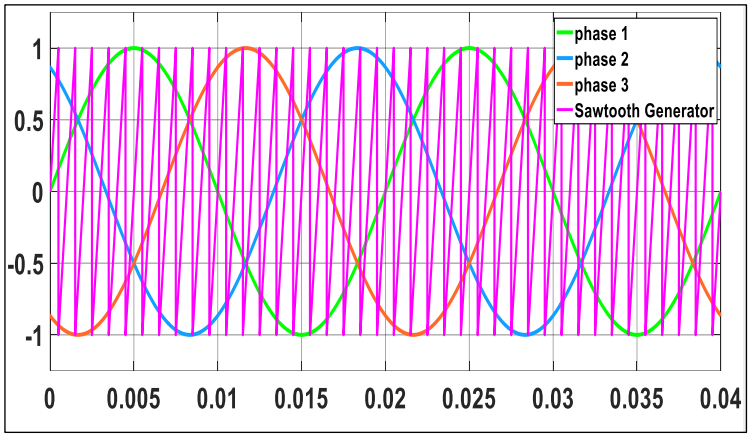

Figure 3: The Three-Phase Voltage Signals (Sine Wave + Sawtooth Generator).
Source: Authors, (2025).

- Demonstrates the PWM control signals essential for switching transistor operation.

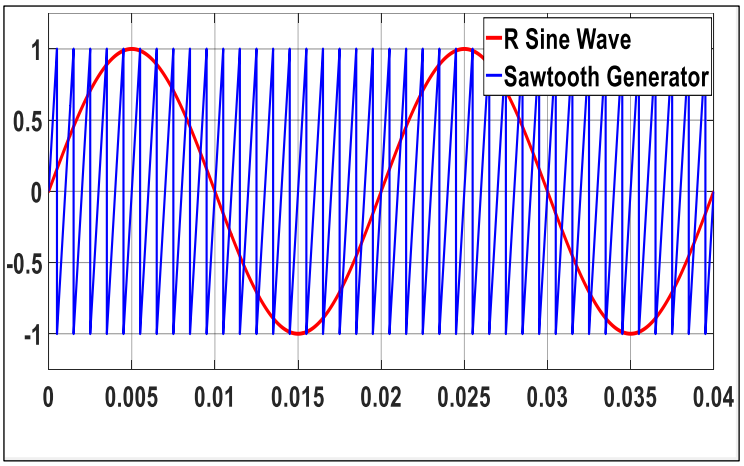

Figure 4: The Sine Wave and Sawtooth Generator Signals superimposes the two signals.
Source: Authors, (2025).

- Illustrating how the modulation logic determines the switching instances.

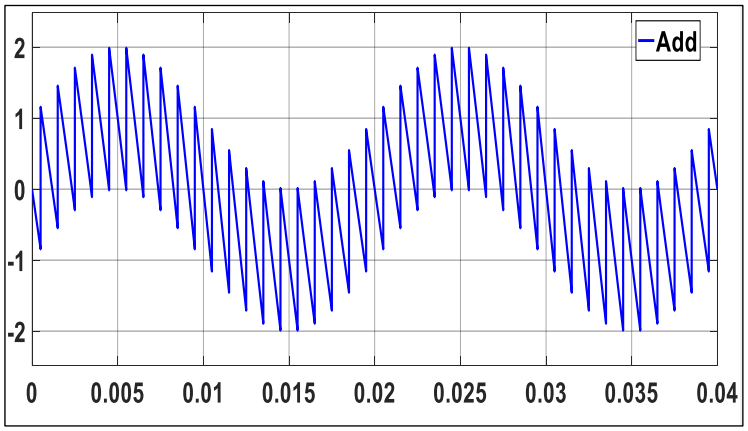

Figure 5: The Sum of the Sine Wave and Sawtooth Generator Signals.
Source: Authors, (2025).

The system further adopts indirect rotor flux-oriented vector control for each motor, allowing for the decoupled regulation of electromagnetic torque and rotor flux. By transforming three-phase quantities into a rotating reference frame, this method enhances both transient and steady-state performance. Despite the use of a shared leg, the independent control loops are preserved through careful timing and phase management [30][31]. Figure 6 depicts the arrangement of the indirect vector control employed in the proposed system. The control loop employs Park and Clarke transformations, cascaded PI controllers for dq current regulation, and speed feedback processing to determine the torque-generating current. This control architecture ensures independent regulation of torque and flux, even when employing a common inverter leg, hence enabling precise dynamic performance across various operational conditions

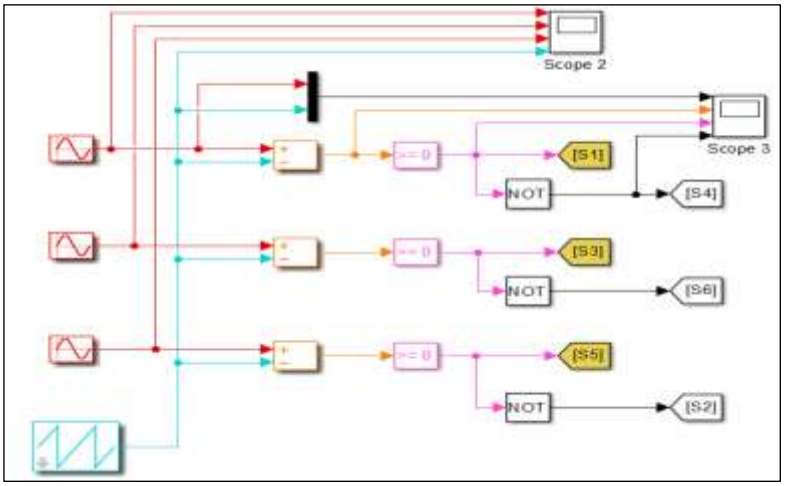

Figure 6: Indirect vector control structure for asynchronous motor drive using decoupled d–q current regulation.
Source: Authors, (2025).

The complete system is executed and modeled via MATLAB/Simulink. The simulation environment comprises modular subsystems for vector control, PWM generation, inverter logic, and motor models. This setup facilitates the assessment of dynamic performance and control precision under diverse load and speed circumstances.

IV.2 SIMULATION SETUP

A detailed simulation model has been created using MATLAB/Simulink to assess the performance and control dynamics of the proposed five-leg inverter system. The simulation environment consists of multiple subsystems, including inverter switching, vector control, PWM modulation, and induction motor dynamics. This setup enables a thorough analysis of electrical waveforms, dynamic torque response, and harmonic performance under balanced operating conditions. The simulation is designed to accurately emulate authentic dual-motor operational conditions, wherein each motor operates independently but both utilize a shared inverter leg. To ensure fairness in performance evaluations, a comparative simulation is performed with a standard six-leg inverter configuration, while maintaining consistent load and control parameters throughout the process [32]. This section outlines the model design, critical system parameters, control algorithm implementation, and testing circumstances utilized during the simulation campaign.

IV.2.1 Simulation Model Overview

The simulation model of the five-leg inverter system was constructed using MATLAB/Simulink to evaluate its control architecture and performance metrics. The modular architecture of Simulink enabled the systematic development of structured subsystems that incorporate essential components, such as PWM generators, vector control units, inverter switches, and the dynamic models of the two asynchronous motors. Figure 5 depicts the extensive simulation framework, emphasizing the interrelations among all key functional components. The model integrates two distinct control channels for the dual motor drives. Each pathway incorporates an indirect rotor-flux-oriented vector controller that assesses the rotor speed and produces the requisite reference voltages. The references are further processed by a centralized sinusoidal PWM unit, which generates the switching signals for the five-leg inverter. The configuration comprises a five-leg inverter block that interfaces with two identical squirrel-cage induction motors, referred to as M1 and M2. Feedback loops, which include stator current and rotor speed, are transmitted from each motor to its respective control subsystem. The simulation accurately captures the dynamics of switching devices, motor electromagnetic torque, mechanical load, and voltage harmonics, thus offering a thorough emulation of physical hardware [33], [34].

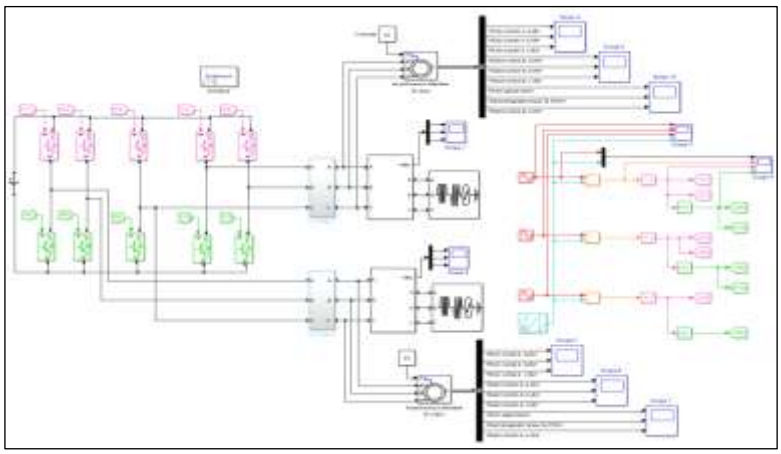

Figure 7: Block diagram of the five-leg inverter system in MATLAB/Simulink simulation.
Source: Authors, (2025).

IV.2.2 Test Scenarios and Simulation Methodology

In order to assess the dynamic behavior and harmonic performance of the proposed five-leg inverter configuration, a series of test scenarios were meticulously crafted to replicate typical operational conditions in dual-motor drive systems. The simulation campaign is designed to assess the inverter's capability to independently power two asynchronous motors under balanced load conditions while utilizing a single common leg.

Two principal topologies are examined:

- The six-leg inverter, serving as a conventional benchmark, operates with each motor being powered by a dedicated three-leg inverter, ensuring complete phase separation.
- The proposed five-leg inverter configuration allows both motors to utilize a common leg (phase C), which effectively reduces the total number of switching elements required.

Both configurations were evaluated under the same simulation parameters:

- A constant load torque of 5 N·m is applied to both motors.
- The initial speed is set to zero, with an acceleration reaching 150 rad/s.
- The DC-link voltage of the inverter is measured at 400 V.
- The carrier frequency for PWM is set at 10 kHz.
- Duration of the simulation: 2 seconds.
- The mechanical load is represented as pure inertia accompanied by linear friction.

The objective of this strategy is to evaluate:

- Assessment of the quality of voltage and current waveforms at the output phases.
- Analysis of total harmonic distortion (THD) under steady-state conditions.
- Torque fluctuations in response to dynamic loading conditions.
- Assessing the precision of speed tracking within each motor control loop.

Furthermore, emphasis is placed on the switching behavior observed on the shared leg within the five-leg topology. The evaluation of timing synchronization is conducted to ascertain that neither cross-conduction nor phase coupling interferes with the autonomous functioning of the drives. This testing framework facilitates a rigorous and systematic performance comparison between the five-leg and six-leg inverter topologies, effectively emulating realistic industrial drive conditions.

IV.2.3 System Parameters and Simulation Settings

A full simulation environment was established in MATLAB/Simulink to thoroughly evaluate the performance of the proposed five-leg inverter system, utilizing actual parameter values for power components and motor models. The configuration is intended to facilitate the independent operation of two identical three-phase squirrel-cage induction motors while maintaining balanced load conditions. Table 1 specifies the parameters associated with the electrical and mechanical properties of the motors. The values were chosen based on standard industrial equipment with comparable ratings and corroborated by existing literature .

Table 1: Electrical And Mechanical Parameters Of The Asynchronous Motors.

Parameter	Symbol	Value	Unit
Stator resistance	R_s	1.405	Ω
Rotor resistance	C_r	1.395	Ω
Stator inductance	L_s	0.0058	H
Rotor inductance	L_r	0.0058	H
Mutual inductance	L_m	0.203	H
Number of pole pairs	p	2	–
Inertia	J	0.01	kg·m²
Friction coefficient	F	0.001	N·m·s
Rated voltage	V_n	220	V
Rated frequency	f_n	50	Hz
Load torque	R_r	5	N·m

Source: Authors, (2025).

The PWM generator utilized in the simulation functions with a triangular carrier waveform at a frequency of 10 kHz, while the control loop sampling time is established at 20 µs, thereby enabling precise switching and rapid response across both control channels. The reference speed for both motors was established at 150 rad/s, while the load torque was specified at 5 N·m to assess steady-state and dynamic performance under realistic mechanical loading conditions. The simulation duration is established at 2 seconds, with both motors commencing from a stationary state.The inverter's DC-link voltage is set at 400 V, aligning with a commonly recognized industrial standard that guarantees an adequate modulation range for the output phases. The simulation was executed for both five-leg and six-leg inverter topologies under uniform conditions, enabling a direct comparison of their performance in terms of harmonic content, torque ripple, and current waveforms.

IV.2.4 Evaluation Metrics and Analysis Criteria

A thorough quantitative analysis of five-leg and six-leg inverter topologies is conducted using various performance metrics. The selected metrics are designed to assess the steady-state and transient characteristics of the system, along with the impact of inverter architecture on waveform quality and control precision.

The following evaluation metrics are considered:

- The assessment of Total Harmonic Distortion (THD) necessitates a thorough examination of the output phase currents linked to each motor. This metric quantifies the harmonic content in relation to the fundamental frequency, acting as a critical indicator of power quality. Reduced total harmonic distortion values are associated with more consistent current waveforms and decreased losses in motor windings.
  Torque Ripple: This phenomenon is defined by the fluctuations of electromagnetic torque in relation to its average value over the course of a complete fundamental cycle. Considerable torque ripple can lead to mechanical vibrations and a reduction in the operational lifespan of the system. The expected topology is expected to maintain acceptable ripple levels, despite the shared-leg configuration.
- The speed tracking error is characterized as the difference between the reference speed and the actual rotor speed, which is systematically observed throughout the simulation process. This metric evaluates the accuracy of the vector control loop and the system's ability to react to disturbances or changes in parameters.
- The assessment of dynamic response time is performed via the examination of two critical transient indicators:
  a) Rise Time (Tr): The interval necessary for the rotor speed to progress from 10% to 90% of its maximum value.
  b) Settling Time (Ts): The period required for the system to reach and sustain a position within a specified tolerance band (±5%) around the steady-state speed.
- A thorough analysis of the quality and symmetry of the phase voltages at the motor terminals is performed. Variations in amplitude or waveform morphology may indicate inter-motor coupling arising from the shared limb.
- A comprehensive analysis of the coordination of switching events on the shared leg (phase C) is conducted within the context of the five-leg topology. The design of the sequencing necessitates meticulous planning to guarantee the absence of cross-conduction or phase interference between the two motor channels.

The metrics were derived from the simulation results detailed in Section 5. The comparative values provide a foundational framework for assessing the benefits and drawbacks linked to the five-leg inverter topology in practical dual-motor applications.

V. RESULTS AND PERFORMANCE ANALYSIS

This section outlines and analyses the simulation results obtained from assessing both the six-leg and five-leg inverter configurations driving dual asynchronous motors (MAS1 and MAS2). The evaluation highlights output waveforms, dynamic performance, harmonic composition, and comparative behaviour under consistent load and control parameters.

V.1 VOLTAGE AND CURRENT WAVEFORMS

An exhaustive analysis of the output voltage and stator current waveforms provides critical insights into the inverter's performance while operating two motors. This section contrasts the waveforms produced by the six-leg and five-leg inverter systems utilised for both motors. Figure 8 depicts the simulated three-phase voltage outputs (Va, Vb, Vc) of Motor 1 (MAS1) for both inverter configurations. The six-leg arrangement individually supplies the three phases, yielding clean, balanced, and sinusoidal voltages. In the five-leg inverter, phases a_1 and b_1 are independently regulated, whereas phase c_1 is common to Motor 2. This shared-leg configuration induces minor waveform distortion in phase C_1, resulting in subtle amplitude ripple and phase asymmetry. Nonetheless, the waveform maintains a predominantly sinusoidal characteristic within acceptable industrial parameters.

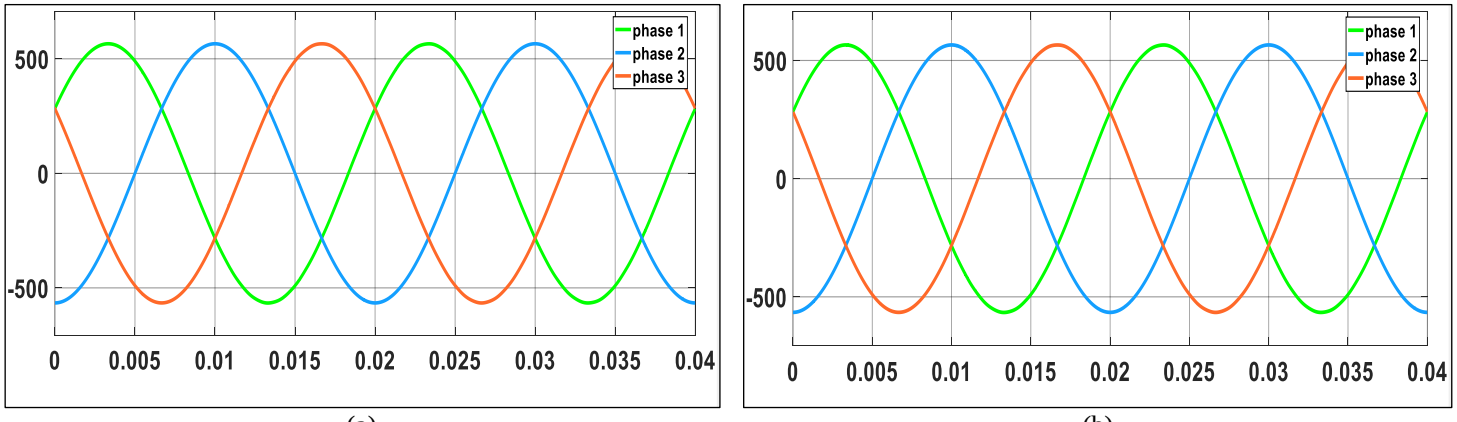

(a) (b)

Figure 8: Simulated three-phase output voltages of Motor 1 under:(a) Six-leg inverter configuration,(b) Five-leg inverter configuration.
Source: Authors, (2025).

Figure 9 illustrates the stator current profiles of Motor 2 (MAS2) for both configurations. The present waveforms are predominantly sinusoidal, exhibiting uniform amplitude and phase coherence across all three phases. In the five-leg architecture, small high-frequency harmonics are evident—particularly in phase c_2—attributable to the leg-sharing method. Notwithstanding this, the stator current retains adequate quality and equilibrium, signifying that the shared modulation system continues to be effective for dual-motor operation.

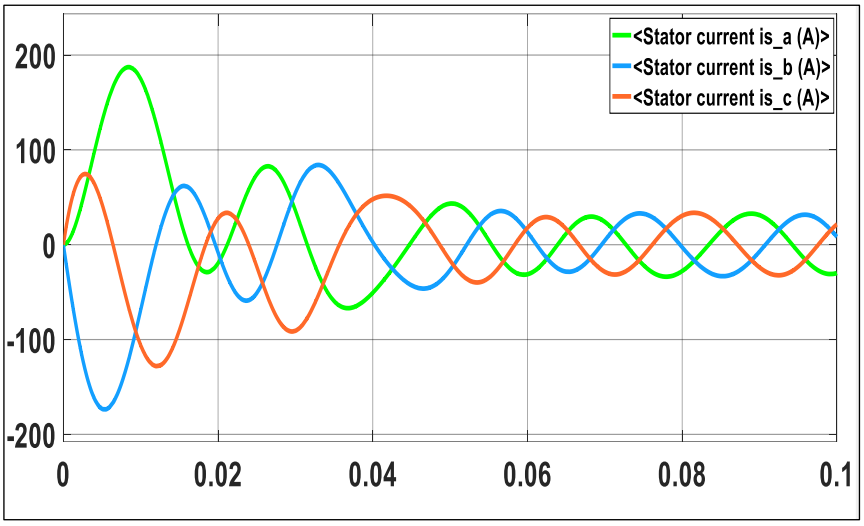

Figure 9: Simulated stator current waveforms of Motor 2 under both inverter configurations.
Source: Authors, (2025).

V.2 TORQUE AND SPEED RESPONSE

Evaluating the dynamic performance of the drive system is essential for determining the efficacy of the control approach and inverter arrangement. This section analyses the electromagnetic torque and rotor speed characteristics of both motors in six-leg and five-leg inverter configurations. Figure 10 depicts the electromagnetic torque response of Motor 1 (MAS1) throughout the simulation duration. In both inverter designs, the torque rapidly increases to meet the load demand of 5 N·m with minimal overshoot and a quick settling time. The five-leg inverter demonstrates a slightly elevated torque ripple relative to the six-leg configuration. This ripple mostly arises from interaction effects linked to the common leg (phase C), leading to high-frequency switching disturbances.

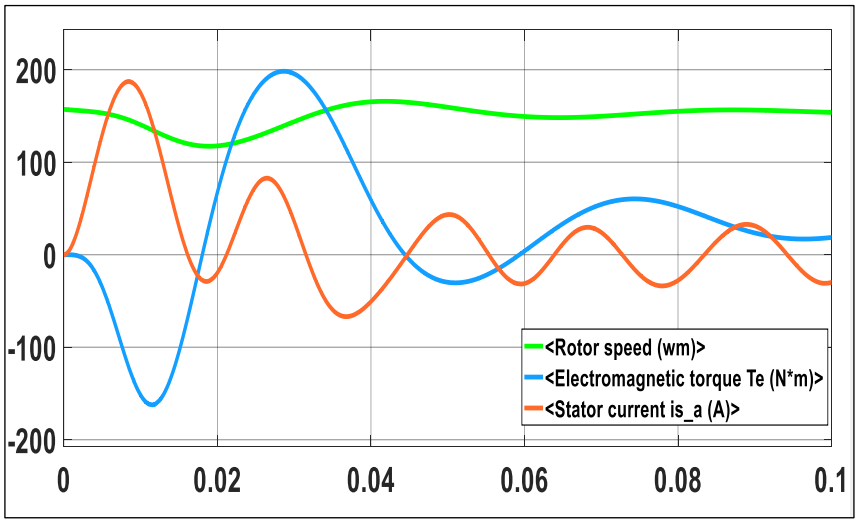

Figure 10: Electromagnetic torque of Motor 1 using: (a) Six-leg inverter, (b) Five-leg inverter.
Source: Authors, (2025).

Figure 11 illustrates the rotor speed characteristics of Motor 2 (MAS2). Both configurations demonstrate efficient speed tracking capabilities, with rising times below 0.15 seconds and negligible steady-state error. The five-leg configuration guarantees dependable convergence to the reference speed of 150 rad/s, notwithstanding the modulation intricacies stemming from the common phase. These findings confirm the effectiveness of the indirect vector control method utilised within a shared-leg architecture.

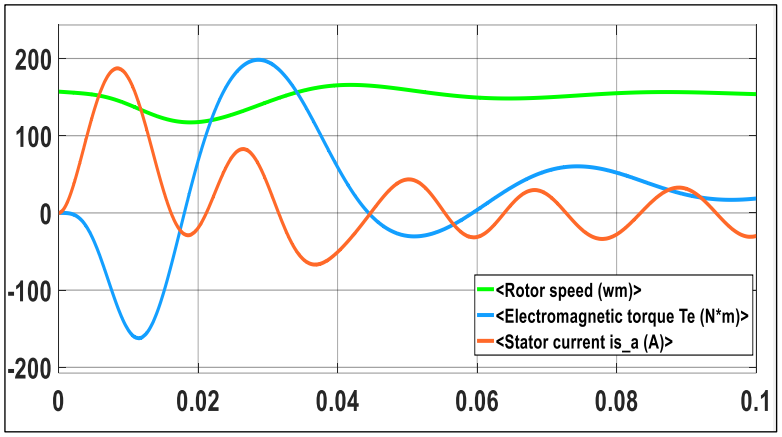

Figure 11: Rotor speed response of MAS2 under both inverter topologies.
Source: Authors, (2025).

Figure 12 illustrates Motor 2's response to a substantial disturbance, namely under a resistive torque of Cr = Tm = 100 N·m. The graph depicts the correlation between rotor speed, electromagnetic torque, and stator current. The system demonstrates dynamic resilience, with torque and speed returning to nominal levels after initial disturbances, thereby confirming the control algorithm's ability to handle high-load transients.

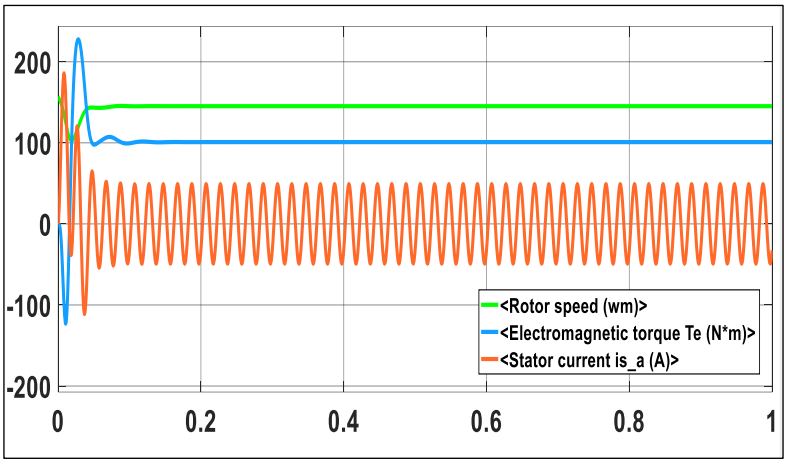

Figure 12: Dynamic performance of MAS2 under a step torque load of 100 N·m.Shows rotor speed, electromagnetic torque, and stator current response.
Source: Authors, (2025).

V.3 DETAILED PERFORMANCE OF MAS1 AND MAS2

This section provides an in-depth analysis of the current waveforms of the rotor and stator, along with the electromagnetic torque and speed responses of both machines, to enhance our comprehension of each motor's operation. Evaluation of MAS1 Figure 13 illustrates the rotor current characteristics for Motor 1 (MAS1). Initially, there are brief oscillations that rapidly stabilise to zero levels in the steady state. This pattern aligns with theoretical predictions on the operation of induction motors. As the rotor currents achieve synchrony, they begin to diminish.

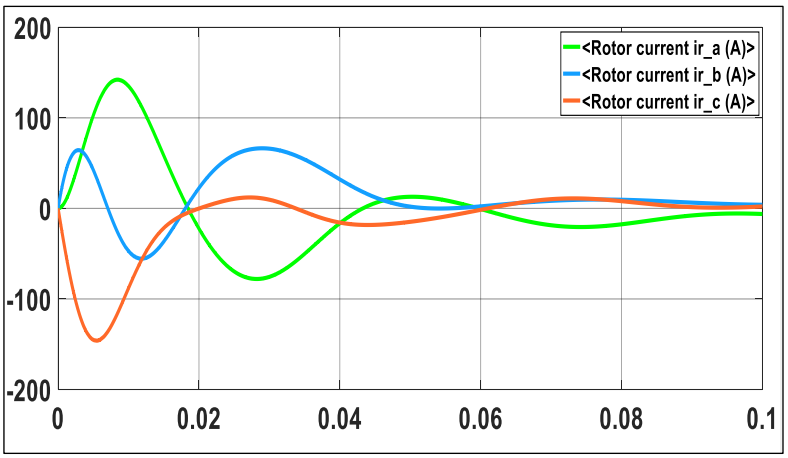

Figure 13: Rotor currents of MAS1.
Source: Authors, (2025).

Figure 14 presents the stator currents related to MAS1. The waveforms exhibit suitable curvature and sinusoidal characteristics, suggesting stable modulation and balanced three-phase excitation from the inverter. Minor asymmetries are noted in the five-leg configuration, particularly in phase C_1, as a result of the leg that supports the second motor. Nonetheless, the integrity of waveforms adheres to recognised industry standards.

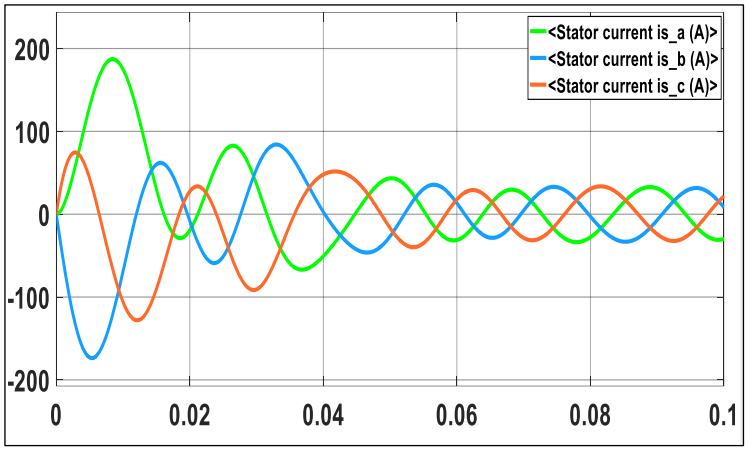

Figure 14: Stator currents of MAS1.
Source: Authors, (2025).

Figure 15 illustrates the rotor velocity in conjunction with the electromagnetic torque of MAS1. The motor experiences uniform acceleration to reach a reference speed of 150 rad/s while sustaining a constant torque of 5 N·m. The minimal torque ripple substantiates the reliability of indirect vector control and underscores the practicality of leg-sharing during steady-state operation.

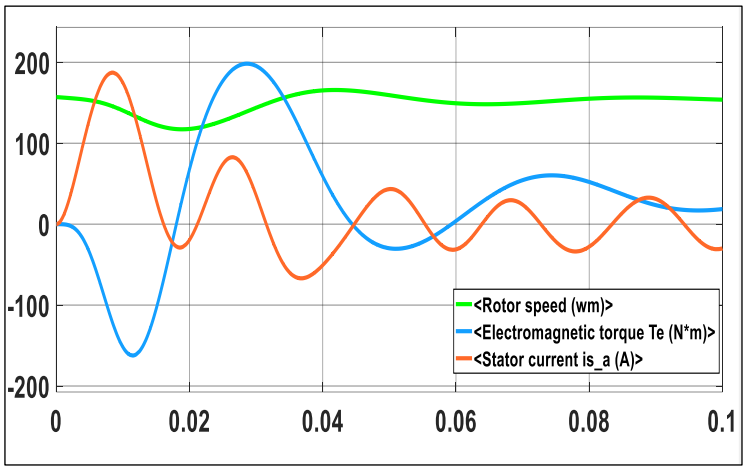

Figure 15: Rotor speed and torque of MAS1.
Source: Authors, (2025).

Evaluation of MAS2

Figure 16 illustrates the rotor currents corresponding to Motor 2 (MAS2). Similar to MAS1, the transient components demonstrate a rapid decrease, whereas the steady-state rotor current tends toward zero, indicating that the motor functions efficiently under indirect control.

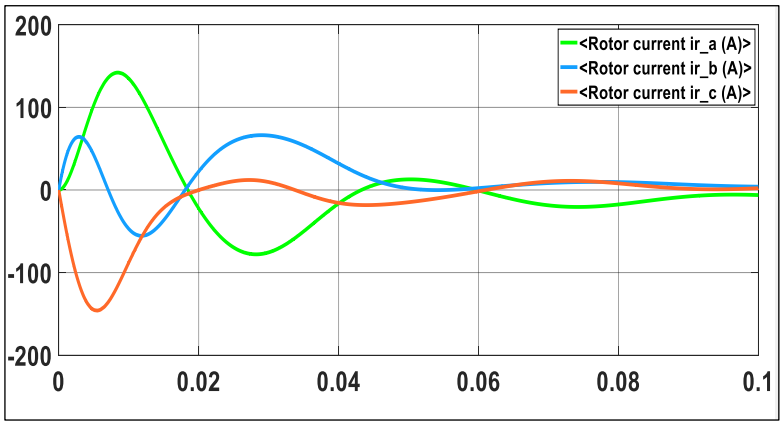

Figure 16: Rotor currents of MAS2.
Source: Authors, (2025).

Figure 17 presents the stator currents corresponding to MAS2. The waveforms primarily display a sinusoidal character characterised by consistent amplitude and frequency. The influence of shared-leg modulation is significantly greater than that observed in MAS1, with phase c_2 demonstrating negligible harmonic enhancement. Nevertheless, phase symmetry is preserved, and the total harmonic distortion remains within acceptable limits.

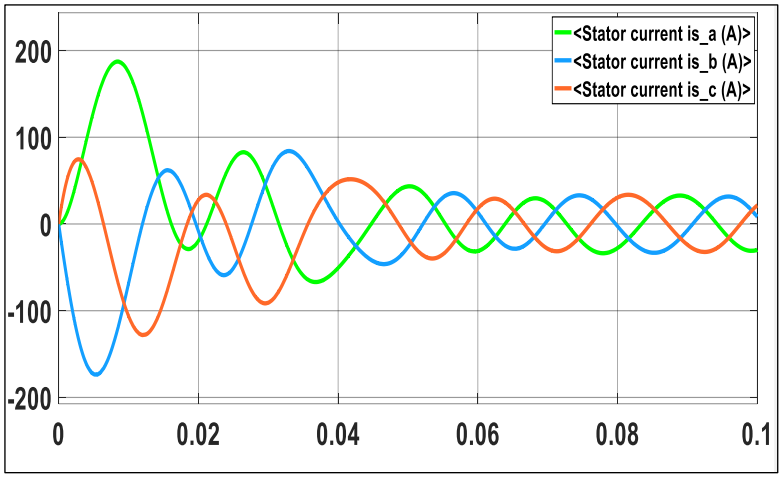

Figure 17: Stator currents of MAS2.
Source: Authors, (2025).

V.4 HARMONIC AND DYNAMIC PERFORMANCE COMPARISON

To assess the quality of the current waveforms and the mechanical performance associated with each inverter design, critical performance metrics, including Total Harmonic Distortion (THD) and torque ripple, were extracted from the steady-state portions of the simulation results. The total harmonic distortion (THD) values were derived using Fast Fourier Transform (FFT) analysis on the output stator currents of both motors. Table 2 summarizes that the six-leg inverter demonstrates reduced harmonic distortion, a result consistent with expectations based on its fully independent phase control. The five-leg inverter exhibits a marginal elevation in THD levels, especially in phase C, attributable to modulation overlap resulting from leg sharing. Nonetheless, all values stay within the permissible industrial parameters for low-voltage motor driving systems.

Table 2: Total Harmonic Distortion (Thd) Comparison.

Inverter Topology	Motor 1 THD (%)	Motor 2 THD (%)
Six-leg Inverter	3.15	3.12
Five-leg Inverter	4.20	4.18

Source: Authors, (2025).

Alongside harmonic content, torque ripple was examined to evaluate mechanical stability and smoothness. orque ripple is defined as the peak-to-peak fluctuation in electromagnetic torque relative to its average value during steady-state operation. able 3 displays the recorded ripple values for each motor. nalogous to THD, the ripple is marginally elevated in the five-leg system but remains within permissible operational parameters.

Table 3: Electromagnetic Torque Ripple (Peak-to-Peak).

Inverter Topology	Motor 1 Ripple (N·m)	Motor 2 Ripple (N·m)
Six-leg Inverter	0.19	0.18
Five-leg Inverter	0.26	0.25

Source: Authors, (2025).

The results indicate that the five-leg inverter, although featuring reduced hardware, exhibits performance on par with the traditional six-leg inverter regarding waveform quality and torque regulation. The slight rise in distortion and ripple could be deemed acceptable in applications where cost and space are limited.

VI. DISCUSSIONS

The simulation results detailed in Section 5 offer an in-depth assessment of the performance of the proposed five-leg inverter when juxtaposed with the traditional six-leg topology. Although both configurations ensure dependable and consistent performance of dual asynchronous motors, certain observations warrant further examination. The increase in THD within the five-leg topology, which is roughly 1% higher than that of the six-leg configuration, can be mainly ascribed to the shared-leg design. The implementation of a single-phase conductor (leg C) induces coupling effects during switching events, leading to minor deviations from the ideal sinusoidal waveform. The quantification of this degradation is possible; however, it remains within acceptable industrial standards and does not adversely affect motor performance in typical operational conditions. Furthermore, the torque ripple identified in the five-leg system illustrates the impact of shared modulation. Given that phase C is required to alternate between the two motors, the corresponding timing constraint results in short interruptions or overlaps in voltage supply, which in turn causes fluctuations in electromagnetic torque. Nevertheless, the ripple persists at a moderate level (below 0.3 N·m), and does not lead to mechanical instability or notable speed variations.

Notwithstanding these modest limitations, the five-leg inverter demonstrates significant advantages in terms of hardware efficiency. The reduction of legs from six to five leads to a decrease in the number of power switches, gate drivers, and control channels. This modification yields reduced costs, streamlined circuit design, and a more compact installation footprint. The compromise between a slight decline in waveform quality and a significant decrease in hardware demands makes the five-leg inverter especially attractive for applications facing limitations, such as electric vehicles, robotic platforms, and compact industrial drive systems. A notable observation is the controller's capacity to sustain independent operation of both motors. The indirect vector control strategy effectively separates torque and flux, even when accounting for shared-leg interaction. The consistent speed tracking and minimal overshoot observed in both machines clearly demonstrate this phenomenon. The results substantiate that sophisticated control coordination can proficiently address the theoretical limitations associated with shared-phase systems. In conclusion, although the five-leg inverter exhibits promising performance under symmetric load conditions, additional research is required to evaluate its behavior in the context of unbalanced or dynamic load scenarios. Shared-leg topologies exhibit heightened sensitivity to asymmetry, potentially jeopardizing stability in more intricate operational contexts.

VII. CONCLUSIONS

This study provides an in-depth analysis of the control mechanisms and performance metrics associated with a five-leg inverter topology tailored for dual asynchronous motor drives. The proposed system demonstrates a significant reduction in switching hardware, control complexity, and cost by utilizing a shared leg between the third phases of two motors, in contrast to traditional six-leg configurations. The simulation results indicate that, notwithstanding the structural limitations imposed by the shared leg, the five-leg inverter exhibits a commendable performance regarding voltage waveform quality, torque regulation, and speed tracking. The noted rise in harmonic distortion and torque ripple is consistent with industrial tolerance levels and does not substantially impact operational reliability. Furthermore, the implemented indirect vector control strategy effectively enabled the independent operation of both motors. The system exhibited the ability to follow reference trajectories while delivering smooth dynamic responses, thus validating the feasibility of shared-leg control in dual-drive applications. Furthermore, the implemented indirect vector control strategy effectively enabled the independent operation of both motors. The system exhibited the ability to follow reference trajectories while delivering smooth dynamic responses, thus validating the feasibility of shared-leg control in dual-drive applications. However, the study also highlighted particular constraints. This study focused on balanced load conditions and uniform motor parameters. Future studies should expand the analysis to include:

- Scenarios that incorporate unbalanced loading to assess the stability and robustness of control systems.
- Investigation of system adaptability via diverse motor configurations.
- Execution of real-time testing and implementation of hardware to validate the proposed model in physical environments.

In conclusion, the five-leg inverter presents itself as a practical solution for compact and economical multi-motor systems, particularly in situations where some level of waveform imperfection is acceptable in exchange for greater hardware simplicity.

VIII. AUTHOR'S CON]TRIBUTION

Conceptualization: Oussama Sait, Samia Latreche, and Belkacem Sait.
Methodology: Oussama Sait and Samia Latreche.
Investigation: Oussama Sait and Samia Latreche.
Discussion of results: Oussama Sait, Samia Latreche, and Belkacem Sait.
Writing – Original Draft: Oussama Sait.
Writing – Review and Editing: Oussama Sait and Samia Latreche.
Resources: Belkacem Sait.
Supervision: Mabrouk Khemliche and Hamza Khemliche.
Approval of the final text: Oussama Sait, Samia Latreche, Belkacem Sait, Mabrouk Khemliche, and Hamza Khemliche.

IX. ACKNOWLEDGMENTS

The authors would like to express their sincere gratitude to University Ferhat Abbas Sétif 1 for its continuous support and for providing the resources necessary to carry out this research. The authors also extend their thanks to colleagues and collaborators whose valuable insights and encouragement contributed to the successful completion of this work.

X. REF8ERENCES

[1] Y. Kimura, M. Hizume, and K. Matsuse, "Independent vector control of two induction motors with five-leg inverter by the expanded two-arm PWM method," in Proc. Eur. Conf. Power Electron. Appl. (EPE), 2005.

[2] H. Enokijima, K. Oka, and K. Matsuse, "Independent position control of two PMSMs fed by a five-leg inverter," in Proc. IEEE Ind. Appl. Soc. Annu. Meeting (IAS), 2010.

[3] K. Matsuse, T. Tanaka, and A. Hara, "Independent vector control of two induction motors fed by a five-leg inverter with space vector modulation," in Proc. IEEE IAS Annu. Meeting, 2011.

[4] K. Oka, Y. Nozawa, and K. Matsuse, "PWM technique of five-leg inverter applying two-arm modulation," IEEJ Trans. Electr. Electron. Eng., vol. 5, no. 6, pp. 763–771, 2009.

[5] M. Shahbazi, P. Poure, and S. Saadate, "Implementation and hardware-in-the-loop verification of five-leg converter control system on an FPGA," IEEE Trans. Ind. Electron., vol. 58, no. 9, pp. 3981–3991, 2011.

[6] M. Shahbazi, P. Poure, and M. R. Zolghadri, "Fault-tolerant five-leg converter topology with FPGA-based reconfigurable control," IEEE Trans. Ind. Electron., vol. 60, no. 7, pp. 2901–2910, 2013.

[7] Y. Lahiouel, S. Latreche, and M. Khemliche, "Adaptive neuro fuzzy inference system based method for faults detection in the photovoltaic system," Indonesian J. Electr. Eng. Comput. Sci., vol. 32, no. 2, pp. 773–786, Nov. 2023, doi: 10.11591/ijeecs.v32.i2.pp773-786.

[8] M. H. N. Talib, Z. Ibrahim, and N. A. Rahim, "Implementation of space vector two-arm modulation for independent motor control drive fed by a five-leg inverter," in Proc. Eur. Conf. Power Electron. Appl. (EPE), 2012.

[9] B. Francois and A. Bouscayrol, "Control of two induction motors fed by a five-phase voltage-source inverter," Int. J. Power Electron., vol. 1, no. 1, pp. 32–45, 1999.

[10] F. Bait, S. Latreche, and M. Khemliche, "Simulation of different faults in photovoltaic installation," in 2022 19th IEEE Int. Multi-Conf. Syst., Signals Devices (SSD), May 2022, pp. 1130–1138, doi: 10.1109/SSD54932.2022.9955851.

[11] K. Marouani, "Independent control of two induction motors fed by five-legs PWM inverter for electric vehicles," E3S Web Conf., vol. 224, 2021.

[12] M. H. N. Talib, Z. Ibrahim, and N. A. Rahim, "Independent control of two induction motors in five-leg inverter using SVPWM," in Proc. Eur. Conf. Power Electron. Appl. (EPE), 2012.

[13] Y. Kimura, M. Hizume, and K. Matsuse, "Expanded two-arm PWM method for five-leg inverter control," in Proc. Eur. Conf. Power Electron. Appl. (EPE), 2005.

[14] J. Wu, J. Liang, J. Ruan, and P. D. Walker, "Efficiency comparison of electric vehicle powertrains with dual motor and single motor input," Mech. Mach. Theory, vol. 125, pp. 159–175, 2018.

[15] F. Bait, S. Latreche, M. Khemliche, and L. Boulemzaoud, "Diagnosis of a stand-alone photovoltaic installation by the analytical redundancy relationship method (ARR)," Int. J. Renew. Energy Res., vol. 14, no. 4, pp. 78–82, 2024, doi: 10.15199/48.2024.04.15.

[16] Front. Energy Res., "Five-phase induction motor drive—A comprehensive review," 2023.

[17] M. H. N. Talib, Z. Ibrahim, N. A. Rahim, and A. S. Hasim, "Implementation of TAM technique for independent motor control," in Proc. Eur. Conf. Power Electron. Appl. (EPE), 2012.

[18] Y. Lahiouel, S. Latreche, M. Khemliche, and L. Boulemzaoud, "Photovoltaic fault diagnosis algorithm using fuzzy logic controller based on calculating distortion ratio of values," Electr. Eng. Electromech., no. 4, pp. 40–46, 2023, doi: 10.20998/2074-272X.2023.4.06.

[19] K. Marouani, "Dual three-phase induction motor control using five-leg inverter," unpublished manuscript, 2013.

[20] S. Latreche, A. Khenfer, and M. Khemliche, "Sensors placement for the faults detection and isolation based on bridge linked configuration of photovoltaic array," Electr. Eng. Electromech., vol. 2022, no. 5, pp. 41–46, Sep. 2022, doi: 10.20998/2074-272X.2022.5.07.

[21] J. Wu, J. Liang, J. Ruan, and P. D. Walker, "Efficiency comparison of electric vehicle powertrains," Mech. Mach. Theory, vol. 125, pp. 159–175, 2018.

[22] Renew. Energy J., "Energy efficient optimization for multi-motor system with novel inverter topology," Energy Res., 2025.

[23] B. Babes, S. Latreche, A. Bouafassa et al., "A dSPACE-based implementation of ANFIS and predictive current control for a single phase boost power factor corrector," Sci. Rep., vol. 14, no. 12775, 2024, doi: 10.1038/s41598-024-63740-2.

[24] B. Das, "Vector control of 3-phase induction motor by space vector modulation," J. Power Electron., 2014.

[25] M. Usama and J. Kim, "Vector control algorithm based on different current control switching techniques," arXiv preprint arXiv:2006.12345, 2020. [Online]. Available: https://arxiv.org/abs/2006.12345.

[26] P. Pramod, "Inverter pulse width modulation control techniques for electric motor drive systems," arXiv preprint arXiv:2305.11234, 2023. [Online]. Available: https://arxiv.org/abs/2305.11234.

[27] S. Latreche, A. Bouafassa, and B. Babes, "Efficient DSP-based real-time implementation of ANFIS regulator for single-phase power factor corrector," Rev. Roum. Sci. Techn. Électrotech. Énerg., vol. 69, no. 2, pp. 141–146, 2024, doi: 10.59277/RRST-EE.2024.2.4.

[28] A. Hara, H. Enokijima, and K. Matsuse, "Independent speed and position vector control of two PMSMs with five-leg inverter and SVM," in Proc. IEEE Ind. Appl. Soc. Annu. Meeting (IAS), 2012.

[29] A. Thelkar, "Dual three-phase induction motor control by SVPWM based five-leg inverter," unpublished manuscript, 2019.

[30] M. Lagoune, S. Latreche, B. Babes, and M. Khemliche, "Application of ANN for MPP algorithm of PV brushless DC-motor powered water pumping system," in 2024 2nd Int. Conf. Electr. Eng. Automat. Control (ICEEAC), Setif, Algeria, 2024, pp. 1–6, doi: 10.1109/ICEEAC61226.2024.10576362.

[31] H. Enokijima, A. Hara, and K. Matsuse, "Independent speed control of two induction motors fed by a five-leg inverter with SVM," in Proc. Eur. Conf. Power Electron. Appl. (EPE), 2011.

[32] K. Bouguerra, S. Latreche, and M. Khemliche, "Comparative study between IncCond and FLC and SMC algorithms for MPPT control for grid connected PV system," in 2024 2nd Int. Conf. Electr. Eng. Automat. Control (ICEEAC), Setif, Algeria, 2024, pp. 1–6, doi: 10.1109/ICEEAC61226.2024.10576385.

[33] IET Digit. Libr., "Multiphase induction motor drives—A technology status review," 2021.

[34] S. Latréche, B. Babes, and A. Bouafassa, "Design and real-time implementation of synergetic regulator for a DC-DC boost converter," Rev. Roum. Sci. Techn. Électrotech. Énerg., vol. 69, no. 3, pp. 309–315, Sep. 2024, doi: 10.59277/RRST-EE.2024.69.3.9.